

Article

Experimental Study on Vibration Control of a Submerged Pipeline Model by Eddy Current Tuned Mass Damper

Wenxi Wang ^{1,2}, Dakota Dalton ², Xugang Hua ¹, Xiuyong Wang ^{3,*}, Zhengqing Chen ¹ and Gangbing Song ^{2,*}

¹ Key Laboratory for Bridge and Wind Engineering of Hunan Province, College of Civil Engineering, Hunan University, Changsha 410082, China; wxwang@hnu.edu.cn (W.W.); cexghua@hnu.edu.cn (X.H.); zqchen@hnu.edu.cn (Z.C.)

² Department of Mechanical Engineering, University of Houston, Houston, TX 77204, USA; ddalton94@hotmail.com

³ College of Civil Engineering, Hunan University of Science and Technology, Xiangtan 411201, China

* Correspondence: cexywang@hnust.edu.cn (X.W.); gsong@uh.edu (G.S.); Tel.: +1-832-606-1000 (G.S.)

Received: 4 September 2017; Accepted: 22 September 2017; Published: 25 September 2017

Abstract: Undesirable vibrations occurring in undersea pipeline structures due to ocean currents may shorten the lifecycle of pipeline structures and even lead to their failure. Therefore, it is desirable to find a feasible and effective device to suppress the subsea vibration. Eddy current tuned mass damper (ECTMD), which employs the damping force generated by the relative movement of a non-magnetic conductive metal (such as copper or aluminum) through a magnetic field, is demonstrated to be an efficient way in structural vibration control. However, the feasibility and effectiveness of ECTMD in a seawater environment has not been reported on before. In this paper, an experiment is conducted to validate the feasibility of an eddy current damper in a seawater environment. A submerged pipeline is used as the controlled structure to experimentally study the effectiveness of ECTMD. The dynamic properties of the submerged pipeline are obtained from dynamic tests and the finite element method (FEM). The optimum design of TMD with a linear spring-damper element for a damped primary structure is carried out through numerical optimization procedures and is used to determine the optimal frequency tuning ratio and damping ratio of ECTMD. In addition, the performance of ECTMD to control the submerged pipeline model is respectively studied in free vibration case and forced vibration case. The results show that the damping provided by eddy current in a seawater environment is only slightly varied compared to that in an air environment. With the optimal ECTMD control, vibration response of the submerged pipeline is significantly decreased.

Keywords: eddy current damping; tuned mass damper; submerged pipeline model; vibration control; seawater environment

1. Introduction

Many control devices have been proposed and successfully applied to control onshore civil structures in past decades [1–7]. Nowadays, thousands of kilometers of pipelines have been installed on the seabed to transport oil and gas. Undesirable vibrations of subsea pipelines subjected to the ocean current may cause the fatigue of pipeline structures and shorten their lifecycle [8]. The control devices used to suppress vibration in onshore structures may be unsuitable or may be too hard to implement in a seawater environment. Therefore, an effective control device which can be employed in seawater environments for vibration suppression of subsea pipelines should be developed. Tuned mass damper (TMD) [9] is a traditional passive control device that has been successfully applied in vibration control of civil structures [10–15] and machining processes [16–18], which consists of a spring-mass

system and a damper. When the frequency of the TMD is tuned closely to that of the primary structure, the vibration energy of the primary structure will be transferred to the TMD through the stiffness force and partly dissipated by the damping force [19,20].

In the previous studies, conventional fluid dampers such as viscous oil dampers [21], Magneto rheological (MR) dampers [22] and impact dampers [23,24] are used to dissipate vibration energy in a TMD system. It should be noted that MR dampers are also employed to control the frequency of a semi-active TMD system in real-time [25,26]. Since the friction force always exists in the relative movement between the TMD and the fluid damper, the conventional TMD equipped with a fluid damper is only activated when the acceleration of the controlled structure exceeds a certain value [14,15]. Because the damping force generated by eddy currents is a non-contact force, no friction force exists in the relative movement between the TMD and eddy current damper. Moreover, compared with conventional oil damper, the eddy current damper is insensitive to the change of temperature. In the regard of those points, eddy current dampers have been proposed to provide the additional damping for a TMD system [27,28]. The damping force generated by the eddy currents is proportional to the relative velocity, which can be regarded as a linear viscous damping [27–31]. Some works on the vibration suppression using eddy current tuned mass damper (ECTMD) have been presented. Larose et al. [32] investigated the vibration control of a wind tunnel bridge model using an ECTMD. In their device, the damping ratio of the ECTMD can be adjusted by changing the clearance between the magnet and the aluminum conductive plate. Bae et al. [33] designed an ECTMD to control the vibration of a cantilever beam and proposed a relatively simple method to calculate the damping force provided by eddy currents numerically. For verifying that an ECTMD is an effective way to control a large-scale structure, a large scale ECTMD was designed and constructed to control a large beam structure [34]. Wen et al. [35] installed an ECTMD system on a footbridge to control the human-induced vibration, resulting in the large-amplitude vibrations being suppressed. Bourquin et al. [36] proposed two ECTMDs to control the first two modes of a bridge mock-up and found that the maximum achievable damping is obtained when a desirable viscous damping level is selected. However, the feasibility of using ECTMDs for vibration control in a seawater environment has not been studied before.

In this paper, an underwater experiment is conducted to validate the feasibility of eddy current damping in a seawater environment. A submerged pipeline is employed as the controlled structure to experimentally study the effectiveness of an ECTMD and the dynamic properties of the pipeline are obtained from dynamic tests and the finite element method (FEM). The optimum design of a TMD for the damped primary structure is carried out through numerical search procedures and is used to determine the optimal tuning ratio and damping ratio of the ECTMD. Finally, the effectiveness of an optimal ECTMD to control the submerged pipeline is experimentally demonstrated both in the free vibration case and forced vibration case.

2. Effectiveness of Eddy Current Damping in Seawater

2.1. Eddy Current Damping

Eddy current damping is generated by magnetic inductions. When a conductive plate moves through a stationary magnetic field, or vice versa, eddy currents will appear in the conductive plate to hinder the movement of the conductive plate [24–26], as shown in Figure 1. The strength of the damping depends upon the strength of the magnetic field, the surface area, and conductivity of the conductive plate, and the rate of change of the magnetic flux [29].

2.2. Free Vibration Tests of a Eddy Current Damper in Seawater Environment

As mentioned before, eddy current dampers have been successfully applied in TMD systems as a linear damping source. The key issue for applying ECTMD to control vibrations occurring in subsea pipelines is the validation of the damping effect of eddy currents in a seawater environment.

Studies worked on the application of eddy current damping in a seawater environment have not been reported on before. In this paper, to verify the feasibility of eddy current damping in a seawater environment, the free vibration responses of a cantilever beam are measured in four cases and the damping ratios of each case are calculated.

The experimental setup is shown in Figure 2a–c. A laser displacement sensor is used to collect the response of the cantilever beam and a seawater container is used to carry seawater to simulate the seawater environment. Moreover, an eddy current damping device, as shown in Figure 2d, with two permanent magnets is fixed on the bottom of the water container to provide extra damping force for the cantilever beam. The sample frequency of the laser displacement sensor is set to 100 Hz and the gap between the magnets and the aluminum plate is set to 5 mm.

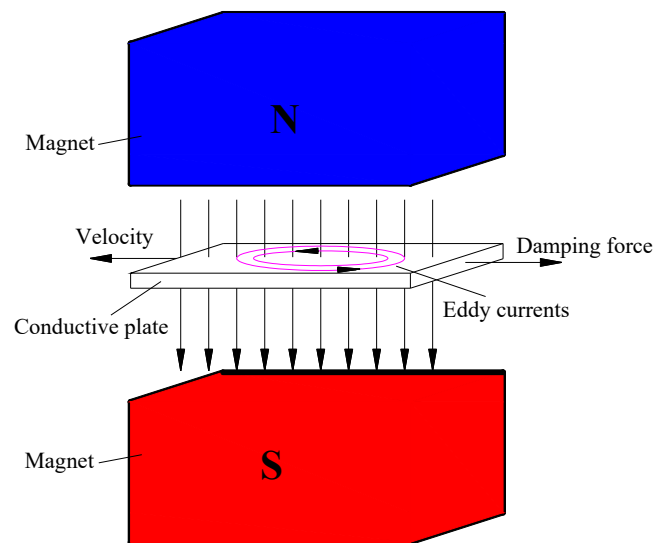
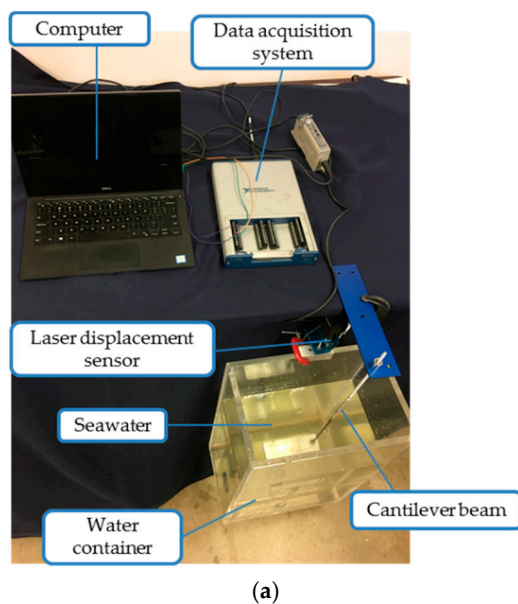
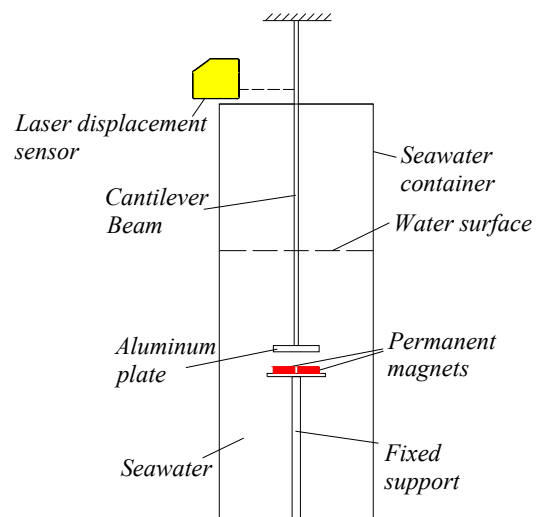


Figure 1. Generation of eddy current damping in a conductive plate.



(a)



(b)

Figure 2. Cont.

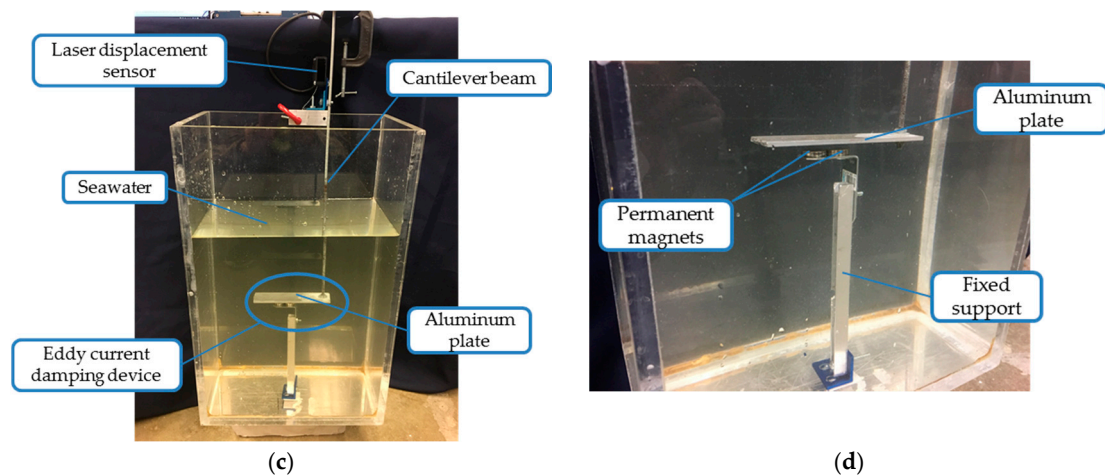


Figure 2. Experimental setup for free vibration tests: (a) global view; (b) side view of seawater container; (c) front view of seawater container; (d) eddy current damper.

2.3. Experimental Results

The free vibration of the cantilever beam is measured in four cases to study the additional damping provided by the eddy currents. Figure 3 plots the free vibration response of the cantilever beam in these four cases. The average damping ratios of the cantilever beam and descriptions of the four cases are given in Table 1. It can be seen that the original damping ratios of the cantilever beam without eddy current damping are 0.55% and 2.87% in the air and in the seawater environment, respectively. The damping ratios with eddy current damping are increased from the original values to 7.33% and 8.98%, respectively. The increased damping ratio provided by eddy current damping is 6.78% in air and 6.02% in the seawater environment. It is shown that the influence of the seawater environment on the eddy current damping is limited and the feasibility of using eddy current damping in seawater is validated.

Moreover, the damping ratio in the first five vibration cycles are obtained from the logarithmic decrement method and plotted in Figure 4. It can be seen that the damping ratio of the cantilever beam at first one or two cycles is larger than that at last few cycles. This phenomenon indicates that the structural damping is much higher during large-amplitude vibration.

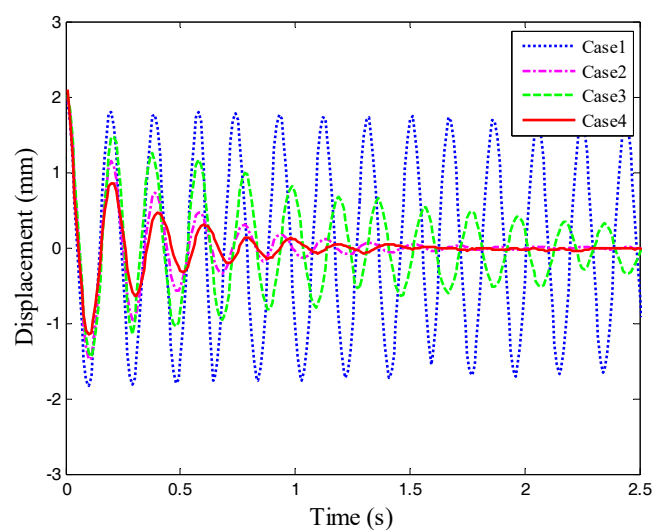


Figure 3. Free vibration response of cantilever beam in each case.

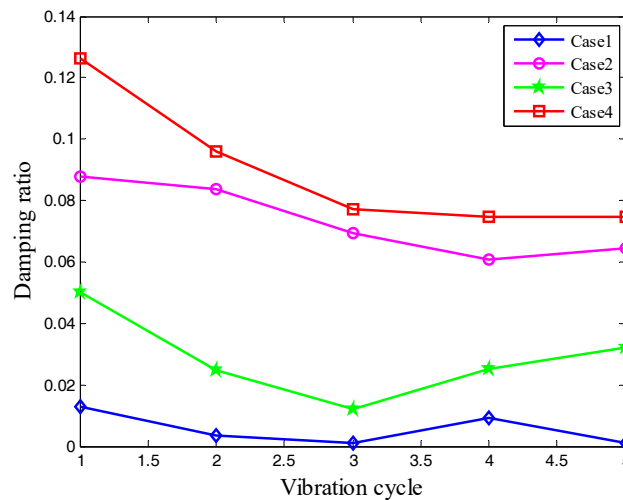


Figure 4. Damping ratio of cantilever beam in the first five vibration cycles.

Table 1. Average damping ratio for each case.

Experimental Case	Case Description	Average Damping Ratio	Increased Damping Ratio
Case1	Without eddy current damping in air	0.55%	In air: 6.78%
Case2	With eddy current damping in air	7.33%	
Case3	Without eddy current damping in seawater	2.87%	In seawater: 6.02%
Case4	With eddy current damping in seawater	8.98%	

3. Experimental Model of a Submerged Pipeline

A submerged pipeline built with polyvinyl chloride (PVC) pipe is used as the controlled structure to verify the effectiveness of an ECTMD in a seawater environment, as shown in Figure 5a. Moreover, the finite element (FE) model of the pipeline shown in Figure 5b is established in ANSYS (11.0, ANSYS Inc., Canonsburg, PA, USA, 2009) and the dynamic properties such as frequency, modal shape, and modal mass are computed. The first vibration mode of the pipeline is selected as the controlled target and the mode shape of this mode is plotted in Figure 5c. The free vibration test of the submerged pipeline is conducted by giving an initial displacement in the middle of the pipeline. Free vibration history is shown in Figure 6a and its Fast Fourier Transform (FFT) amplitude in the frequency domain is plotted in Figure 6b. The dynamic properties of the pipeline are listed in Table 2, which were obtained through experimental testing and FE computation. The modal frequency and modal mass are 3.2 Hz and 0.728 kg, respectively. The vertical damping ratio of the pipeline is 2.4%, which is a relatively high value compared with onshore civil structures.

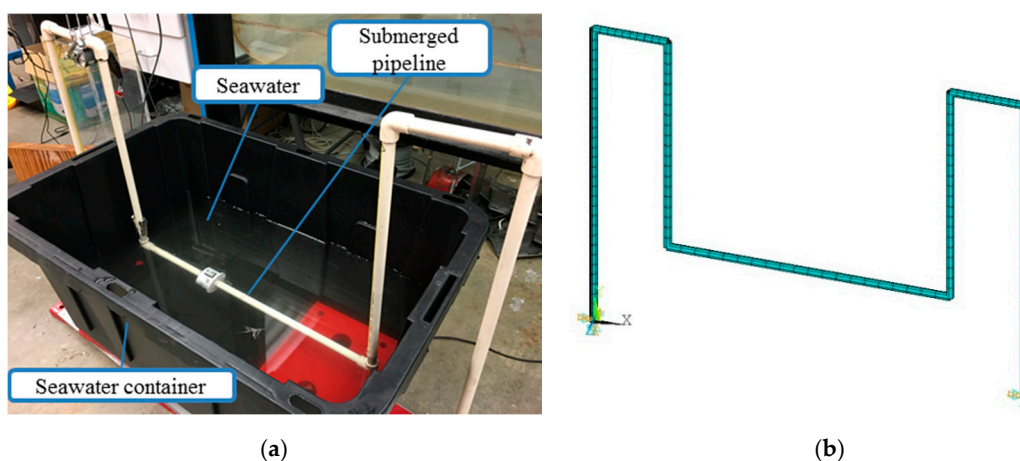


Figure 5. Cont.

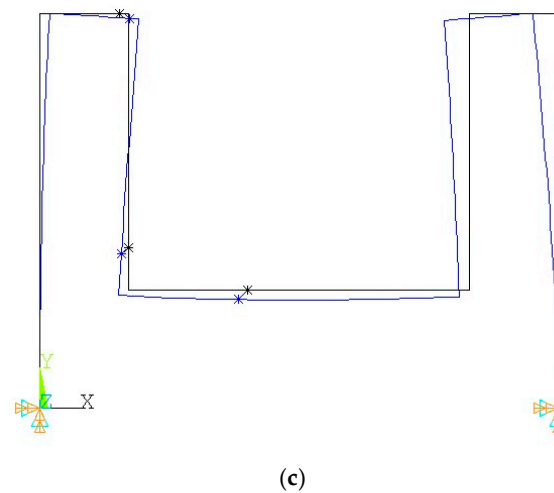


Figure 5. Submerged pipeline model and its finite element model: (a) polyvinyl chloride (PVC) pipeline in the seawater container; (b) finite element (FE) model; (c) first vibration mode shape.

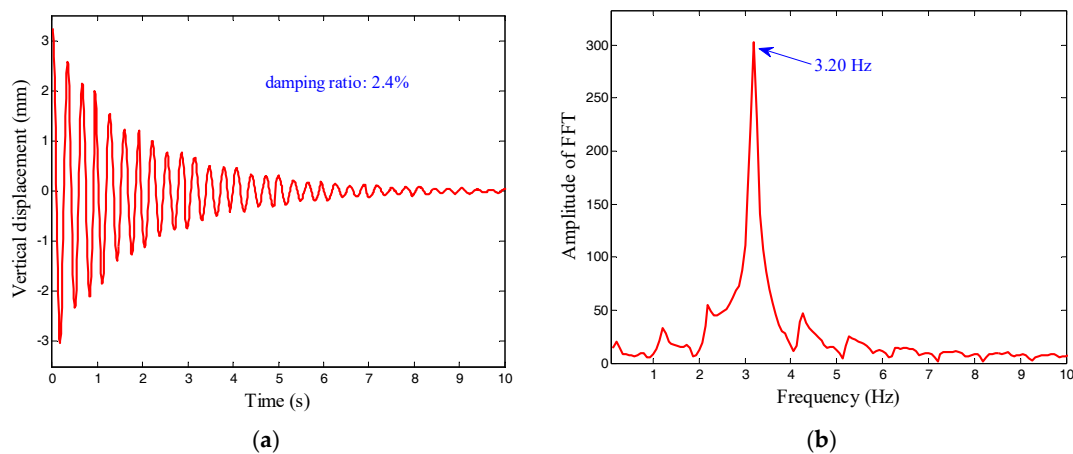


Figure 6. Vertical response and its Fast Fourier transform (FFT) amplitude of the submerged pipeline in seawater environment: (a) free vibration response; (b) FFT amplitude.

Table 2. Modal parameters of the pipeline structure.

Result	Frequency	Damping Ratio	Modal Mass
FE computation	3.26 Hz	-	0.728 kg
Experimental result	3.20 Hz	2.4%	-

4. Optimal Design of ECTMD for Damped Structure

If its tuning ratio and damping ratio is off-tuned, the ECTMD will lose its control efficiency. Due to the eddy current damping being linearly proportional to the relative velocity between ECTMD and the primary structure, the optimization procedures of TMD with a linear viscous damper can be employed to design the optimal parameters of the ECTMD. The optimal tuning ratio and damping ratio of a tuned mass damper (TMD) system for an undamped structure are given by [37],

$$r_{opt} = \frac{1}{1 + \mu} \quad (1)$$

$$\zeta_{opt} = \sqrt{\frac{3\mu}{8(1 + \mu)}} \quad (2)$$

where r_{opt} and ζ_{opt} are the optimal frequency tuning ratio and the optimal damping ratio of the TMD respectively, $\mu = m_{tmd}/m_s$ is the mass ratio of the TMD, m_{tmd} and m_s are the masses of the primary structure and the TMD, respectively.

The damping ratio of the primary structure before a TMD is attached can be calculated by $\zeta_s = c_s/(2m_s(k_s/m_s)^{1/2})$. For a primary structure with a low damping ratio, such as 0.5% or lower, Equations (1) and (2) can be used to design the optimal parameters of TMD. When the damping ratio of the controlled structure is higher than 2%, such as the tested submerged pipeline in the Section 3, the optimal tuning ratio and damping ratio calculated by Equations (1) and (2) may result in detuning to the ECTMD system, and reduce its optimal control ability [38,39]. An optimum design of a TMD for a damped controlled structure is proposed by Thompson [40] using the frequency focus method. This method for finding the optimal parameter of a TMD is relatively complicated. Thompson's work focused on highly damped structures, but the damping ratios of most civil structures are under 5%. Therefore, the optimal parameters of a TMD system for damped structures based on H_∞ optimization method are studied in this paper. The equation of motion of the damped structure with a linear TMD control, as shown in Figure 7, can be expressed as Equation (3),

$$\begin{cases} m_s \ddot{x}_s + c_s \dot{x}_s + k_s x_s + c_{tmd}(\dot{x}_s - \dot{x}_{tmd}) + k_{tmd}(x_s - x_{tmd}) = f_0 \sin(\omega t) \\ m_{tmd} \ddot{x}_{tmd} + c_{tmd}(\dot{x}_{tmd} - \dot{x}_s) + k_{tmd}(x_{tmd} - x_s) = 0 \end{cases} \quad (3)$$

where m_s , c_s , k_s , x_s are the mass, damping coefficient, stiffness, and displacement of the controlled structure, and m_{tmd} , c_{tmd} , k_{tmd} , x_{tmd} are the mass, damping coefficient, stiffness, and displacement of the TMD. $f_0 \sin(\omega t)$ is the external excitation applied on the controlled structure.

The dynamic magnification factor of the primary structure is defined as $DMF(\omega) = x_{s0}k_s/f_0$, and it can be expressed as Equations (4),

$$DMF(\omega) = \frac{x_{s0}}{f_0/k_s} = \frac{k_s}{\left| (k_s + i\omega c_s - m_s \omega^2) + k_{tmd} + i\omega c_{tmd} - \frac{(k_{tmd} + i\omega c_{tmd})^2}{k_{tmd} + i\omega c_{tmd} - m_{tmd} \omega^2} \right|} \quad (4)$$

where i is complex unit $(-1)^{1/2}$ and x_{s0} is the amplitude of steady-state response. The modal mass ratio, tuning ratio, and damping ratio of TMD are defined as $\mu = m_{tmd}/m_s$, $r = (k_{tmd}/m_{tmd})^{1/2}/(k_s/m_s)^{1/2}$, and $\zeta = c_{tmd}/(2m_{tmd}(k_{tmd}/m_{tmd})^{1/2})$, respectively. The optimization objective function based on H_∞ optimization method is written as Equation (5) [41,42]. It should be noted the objective function is aimed at minimizing the displacement response of the primary structure. The objective function targeted to minimize the acceleration of the primary structure can be found in reference [43].

$$\min_{r, \zeta} \max_{\omega} DMF(\omega) \quad (5)$$

Equation (5) is solved through a numerical optimization and the optimal parameters of the TMD are achieved. The optimal tuning ratio and damping ratio of a TMD for the damped structure from the numerical optimization are shown in Figure 8 along with the optimal parameters obtained from Equations (1) and (2). The mass ratio of TMD μ is varied from 0.01 to 0.1 with an interval of 0.01. It can be observed from Figure 8 that the optimal parameters obtained by the numerical optimization have the same values with the results calculated from Equations (1) and (2) when it is designed for an undamped structure. When the damping ratio of the controlled structure is increased, the optimal tuning ratio of TMD is lower than the value for the undamped structure, and the optimal damping ratio of TMD will increase slightly. The optimal parameters of a TMD for different mass ratios and various damping ratios of primary structures are listed in Table 3.

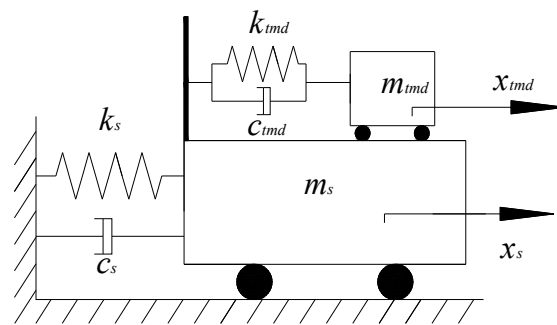


Figure 7. Mechanical model of damped structure with a tuned mass damper (TMD).

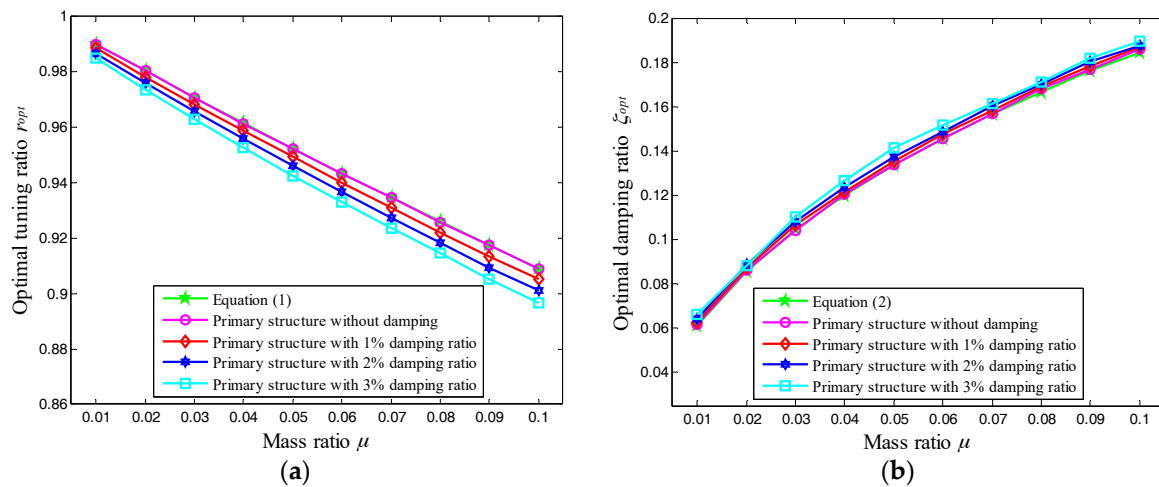


Figure 8. Optimal frequency tuning ratio r_{opt} and damping ζ_{opt} of a TMD for damped structure: (a) optimal frequency tuning ratio; (b) optimal damping ratio.

Table 3. Optimal parameters of a TMD for the damped structure.

Mass Ratio	$\zeta_s = 1\%$		$\zeta_s = 2\%$		$\zeta_s = 3\%$	
μ	r_{opt}	ζ_{opt}	r_{opt}	ζ_{opt}	r_{opt}	ζ_{opt}
$\mu = 0.01$	0.9886	0.0625	0.9869	0.0643	0.9851	0.0662
$\mu = 0.02$	0.9783	0.0874	0.9761	0.0886	0.9738	0.0883
$\mu = 0.03$	0.9684	0.1064	0.9658	0.1084	0.9630	0.1100
$\mu = 0.04$	0.9588	0.1213	0.9558	0.1233	0.9526	0.1268
$\mu = 0.05$	0.9493	0.1355	0.9461	0.1371	0.9426	0.1413
$\mu = 0.06$	0.9401	0.1473	0.9367	0.1488	0.9330	0.1518
$\mu = 0.07$	0.9311	0.1584	0.9274	0.1604	0.9237	0.1614
$\mu = 0.08$	0.9222	0.1691	0.9184	0.1702	0.9145	0.1710
$\mu = 0.09$	0.9135	0.1784	0.9095	0.1805	0.9053	0.1817
$\mu = 0.1$	0.9051	0.1869	0.9010	0.1877	0.8967	0.1896

5. Effectiveness of ECTMD to Control a Submerged Pipeline

In general, the mass ratio of a TMD cannot be too large. Therefore, the mass of the designed ECTMD added on the experimental pipeline structure is 32 g, which means the mass ratio μ is 4.4%. Considering the mass ratio $\mu = 4.4\%$ and the primary damping ratio of the pipeline structure $\zeta_s = 2.4\%$, the optimal tuning ratio and damping ratio of the ECTMD are obtained from Table 3 to be 0.9508 and 12.63%, respectively. For the implementation of the ECTMD, two tiny cantilever beams are used to provide stiffness for the ECTMD and the eddy current damper are utilized to provide the additional damping for the ECTMD. The natural frequency and damping ratio of the ECTMD can be adjusted

through changing the length of the cantilever beams and the gap between the aluminum plates and the magnets. The configuration of the ECTMD and its eddy current damper device for the submerged pipeline are shown in Figure 9. The eddy current damper device consists of two aluminum plates with a thickness of 3 mm and permanent magnets. The ECTMD is installed in the mid-span of the pipeline.

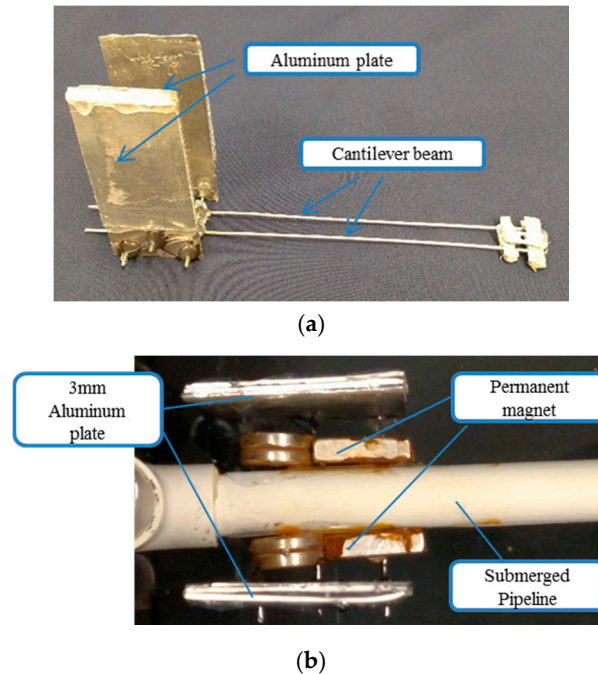


Figure 9. Implementation of the eddy current tuned mass damper (ECTMD) on the pipeline model: (a) configuration of ECTMD; (b) eddy current damper device.

To obtain the fundamental natural frequency and damping ratio of the ECTMD, free vibration tests of ECTMD are conducted in the seawater environment. When the length of the cantilever beam is set to 13.5 cm and the gap between magnets and aluminum plates is set to 4.2 mm, the frequency and the damping ratio is quite close to the optimal values. Figure 10 shows the vertical free vibration history of the ECTMD device with and without magnets, and the frequency responses are also shown in Figure 10. It can be seen that the natural frequency and the damping ratio of the ECTMD without magnets are respectively, 3.07 Hz and 6.1%, in the seawater environment. However, when the permanent magnets are added and eddy current damping is activated, the damping ratio of the ECTMD is sharply increased from 6.1% to 13.9%, which helps the ECTMD to achieve the optimal damping. The parameters of the ECTMD in the experiment are summarized in Table 4.

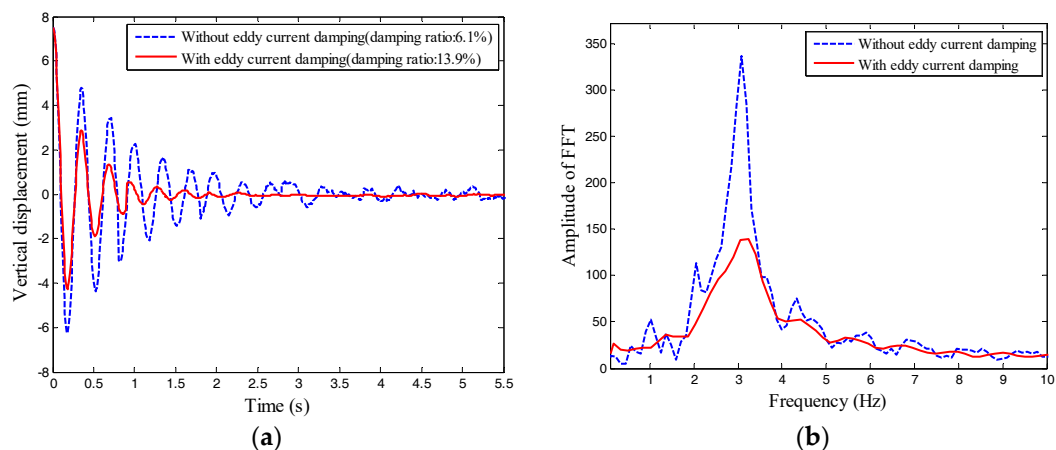


Figure 10. Vertical free vibration history and its response in frequency domain of the ECTMD with and without eddy current damping in seawater: (a) free vibration; (b) FFT amplitude.

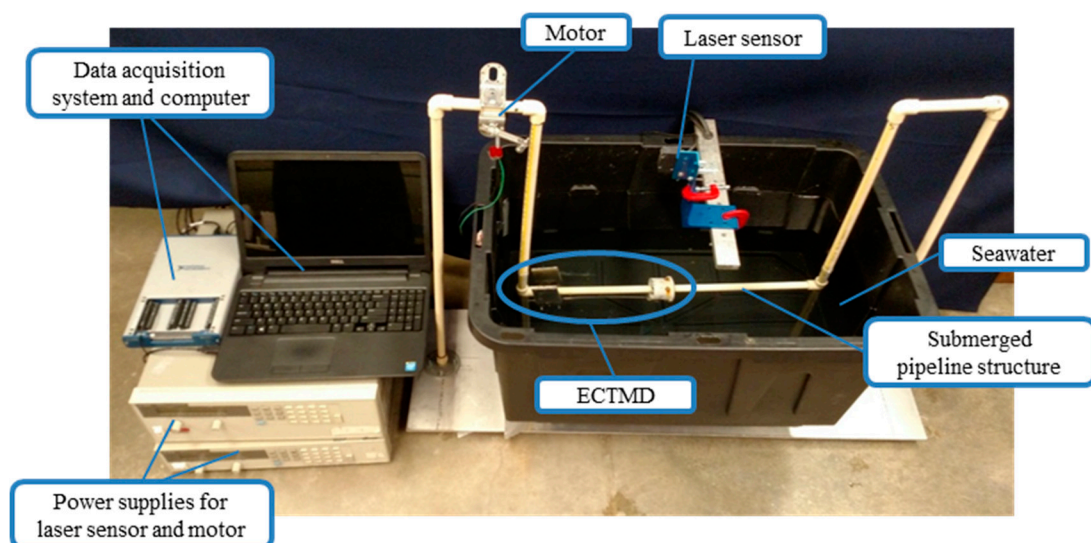
Table 4. Dynamic property of ECTMD.

Case	Mass Ratio	Frequency	Tuning Ratio	Damping Ratio
Target value	4.4%	3.04 Hz	0.9508	12.63%
Experimental value		3.07 Hz	0.9594	13.9%

Figure 11 shows the experimental setup for the testing of the submerged pipeline model. A seawater container is employed to simulate the seawater environment. The pipeline model is submerged 10 cm beneath the surface of the seawater, which is a sufficient depth for the full submersion of the ECTMD during vibration tests. A laser displacement sensor is installed to measure the vertical displacement of the submerged pipeline in the mid-span location. Two different cases, namely structure without control and structure controlled by ECTMD, are tested both in the free vibration and forced vibration case. A motor with unbalanced mass is mounted on the pipeline structure as a harmonic force generator, which can apply harmonic loads in different frequencies by adjusting the input voltage.

Figure 12 plots the vertical response of the pipeline model in free vibration and resonant response. It can be observed that the damping ratio of the vertical vibration is significantly increased from 2.4% to 5.5% when the ECTMD is installed on the pipeline model and the free vibration reduces to zero within 10 periods. The resonant response is reduced by 80.5% while the peak of the no control case is 6.20 mm and the peak with ECTMD control is 1.21 mm. Additionally, the steady-state response in a large frequency range is tested and the vertical response amplitudes is plotted in Figure 13. The results show that the ECTMD can suppress the large amplitude vibration of the submerged pipeline model in a wide frequency range.

The purpose of the current work is aimed to reduce large amplitude vibrations occurred on the subsea pipeline structures. To apply the proposed ECTMD in vibration control of a real environmental setting, the modal parameters such as frequency and modal mass of the vibration mode should be obtained from the finite element model or field test in the design stage. According to the proposed optimization method, the optimal frequency tuning ratio and the optimal damping ratio of the ECTMD can be designed when the modal parameters of a subsea pipeline are already known. In the implementation stage, the configuration of the ECTMD used in the control experiment is worth to be considered. The magnet can be fixed on the pipeline and the aluminum plates can be used as mass. The frequency of the ECTMD will be easily tuned by changing the length of the supporting cantilever beam.

**Figure 11.** Experimental setup for the testing of the submerged pipeline.

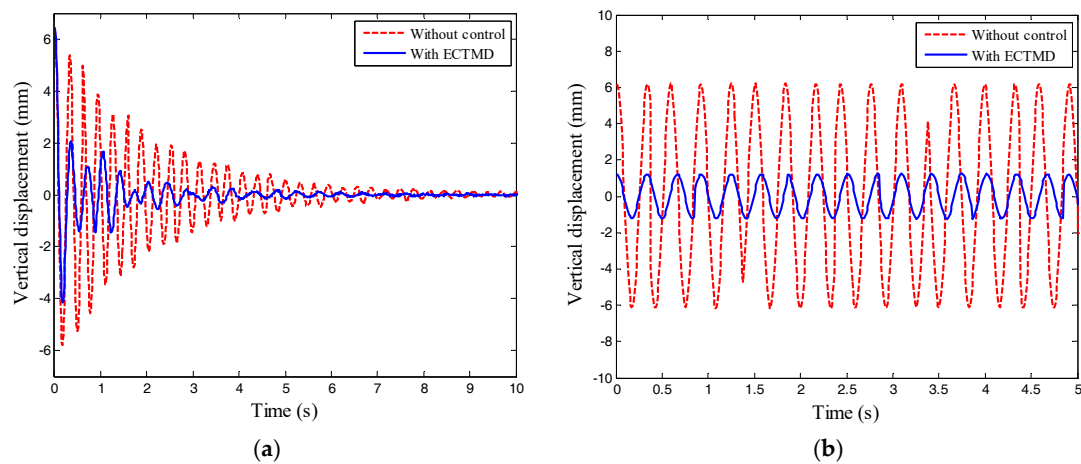


Figure 12. Vertical response of the pipeline model in seawater environments: (a) Free vibration; (b) resonant vibration.

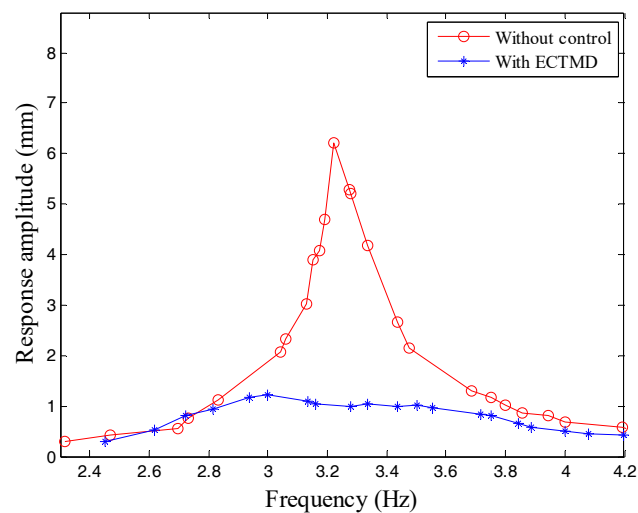


Figure 13. Vertical response of the pipeline model in a large frequency domain.

6. Conclusions

In the present work, a conception of using an ECTMD to control a subsea pipeline structure was introduced. The feasibility experiment was performed to demonstrate that eddy current damping can be used in a seawater environment. To obtain the optimal parameters of a TMD for a damped structure, a numerical optimization method was adopted. Then the attenuation experiments were carried out to show the performance of the ECTMD in a seawater environment.

The results of this study show that eddy current damping can be employed in a seawater environment. The additional damping by eddy currents in the seawater environment is almost the same as in the air environment. As shown from the vibration suppression experiment in the seawater environment, the damping of the submerged pipeline model is increased from 2.4% to 5.5% and the ECTMD can significantly reduce the peak response of the pipeline in a wide frequency range.

Acknowledgments: This research work was supported by the National Key Basic Research Program of China ('973 Project') (Grant Number 2015CB057702) and the Intergovernmental Innovation and Corporation Program of China (Grant Number 2016YFE0127900). The support from the National Natural Foundation of China (Grant Numbers 51422806; 51378203) is also greatly acknowledged. In addition, the first author's research stay at the University of Houston is sponsored by the China Scholarship Council (CSC) and the second author is sponsored by the Summer Undergraduate Research Fellowship at the University of Houston.

Author Contributions: All authors discussed and agreed upon the idea, and made scientific contributions. Wenxi Wang, Zhengqing Chen and Gangbing Song designed the experiments and wrote the paper, Dakota Dalton and Wenxi Wang collected the experimental and analyzed the data, Xugang Hua and Xiuyong Wang performed the optimum design of ECTMD and revised the paper.

Conflicts of Interest: The authors declare no conflict of interest.

References

1. Lu, Z.; Masri, S.F.; Lu, X. Parametric studies of the performance of particle dampers under harmonic excitation. *Struct. Control Health Monit.* **2011**, *18*, 79–98. [[CrossRef](#)]
2. Lu, Z.; Masri, S.F.; Lu, X. Studies of the performance of particle dampers attached to a two-degrees-of-freedom system under random excitation. *J. Vib. Control* **2011**, *17*, 1454–1471.
3. Tian, L.; Rong, K.; Zhang, P.; Liu, Y. Vibration control of a power transmission tower with pounding tuned mass damper under multi-component seismic excitations. *Appl. Sci.* **2017**, *7*, 477. [[CrossRef](#)]
4. Li, H.; Liu, M.; Li, J.; Guan, X.; Ou, J. Vibration control of stay cables of the shandong binzhou yellow river highway bridge using magnetorheological fluid dampers. *J. Bridge Eng.* **2007**, *12*, 401–409. [[CrossRef](#)]
5. Cai, C.S.; Wu, W.J.; Araujo, M. Cable vibration control with a TMD-MR damper system: Experimental exploration. *J. Struct. Eng.* **2007**, *133*, 629–637. [[CrossRef](#)]
6. Jiang, J.; Zhang, P.; Patil, D.; Li, H.; Song, G. Experimental studies on the effectiveness and robustness of a pounding tuned mass damper for vibration suppression of a submerged cylindrical pipe. *Struct. Control Health Monit.* **2017**, e2027. [[CrossRef](#)]
7. Fu, W.; Zhang, C.; Sun, L.; Askari, M.; Samali, B.; Chung, K.L.; Sharafi, P. Experimental investigation of a base isolation system incorporating MR dampers with the high-order single step control algorithm. *Appl. Sci.* **2017**, *7*, 344. [[CrossRef](#)]
8. Biswas, S.K.; Ahmed, N.U. Optimal control of flow-induced vibration of pipeline. *Dyn. Control* **2001**, *11*, 187–201. [[CrossRef](#)]
9. Frahm, H. Device for Damping Vibrations of Bodies. U.S. Patent 989958, 18 April 1911.
10. Tao, T.; Wang, H.; Yao, C.; He, X. Parametric sensitivity analysis on the buffeting control of a long-span triple-tower suspension bridge with MTMD. *Appl. Sci.* **2017**, *7*, 395. [[CrossRef](#)]
11. Li, C. Performance of multiple tuned mass dampers for attenuating undesirable oscillations of structures under the ground acceleration. *Earthq. Eng. Struct. Dyn.* **2000**, *29*, 1405–1421. [[CrossRef](#)]
12. Varadarajan, N.; Nagarajaiah, S. Wind response control of building with variable stiffness tuned mass damper using empirical mode decomposition/Hilbert transform. *J. Eng. Mech.* **2004**, *130*, 451–458. [[CrossRef](#)]
13. Setareh, M.; Hanson, R.D. Tuned mass dampers to control floor vibration from humans. *J. Struct. Eng.* **1992**, *118*, 741–762. [[CrossRef](#)]
14. Caetano, E.; Cunha, Á.; Magalhães, F.; Moutinho, C. Studies for controlling human-induced vibration of the Pedro e Inês footbridge, Portugal. Part 1: Assessment of dynamic behaviour. *Eng. Struct.* **2010**, *32*, 1069–1081. [[CrossRef](#)]
15. Caetano, E.; Cunha, Á.; Moutinho, C.; Magalhães, F. Studies for controlling human-induced vibration of the Pedro e Inês footbridge, Portugal. Part 2: Implementation of tuned mass dampers. *Eng. Struct.* **2010**, *32*, 1082–1091. [[CrossRef](#)]
16. Sims, N.D. Vibration absorbers for chatter suppression: A new analytical tuning methodology. *J. Sound Vib.* **2007**, *301*, 592–607. [[CrossRef](#)]
17. Yang, Y.; Munoa, J.; Altintas, Y. Optimization of multiple tuned mass dampers to suppress machine tool chatter. *Int. J. Mach. Tools Manuf.* **2010**, *50*, 834–842. [[CrossRef](#)]
18. Wang, M.; Zan, T.; Yang, Y.; Fei, R. Design and implementation of nonlinear TMD for chatter suppression: An application in turning processes. *Int. J. Mach. Tools Manuf.* **2010**, *50*, 474–479. [[CrossRef](#)]
19. Kim, S.M.; Wang, S.; Brennan, M.J. Optimal and robust modal control of a flexible structure using an active dynamic vibration absorber. *Smart Mater. Struct.* **2011**, *20*, 045003. [[CrossRef](#)]
20. Weber, F. Semi-active vibration absorber based on real-time controlled MR damper. *Mech. Syst. Signal Process.* **2014**, *46*, 272–288. [[CrossRef](#)]
21. Kwok, K.C.S.; Samali, B. Performance of tuned mass dampers under wind loads. *Eng. Struct.* **1995**, *17*, 655–667. [[CrossRef](#)]

22. Hong, S.R.; Wang, G.; Hu, W.; Wereley, N.M. Liquid spring shock absorber with controllable magnetorheological damping. *Proc. Inst. Mech. Eng. Part D* **2006**, *220*, 1019–1029. [[CrossRef](#)]
23. Wang, W.; Hua, X.; Wang, X.; Chen, Z.; Song, G. Optimum design of a novel pounding tuned mass damper under harmonic excitation. *Smart Mater. Struct.* **2017**, *26*, 055024. [[CrossRef](#)]
24. Lu, Z.; Chen, X.; Zhang, D.; Dai, K. Experimental and analytical study on the performance of particle tuned mass dampers under seismic excitation. *Earthq. Eng. Struct. Dyn.* **2017**, *46*, 697–714. [[CrossRef](#)]
25. Koo, J.H.; Ahmadian, M.; Setareh, M. Experimental robustness analysis of magneto-rheological tuned vibration absorbers subject to mass off-tuning. *J. Vib. Acoust.* **2006**, *128*, 126–131. [[CrossRef](#)]
26. Weber, F.; Maślanka, M. Frequency and damping adaptation of a TMD with controlled MR damper. *Smart Mater. Struct.* **2012**, *21*, 055011. [[CrossRef](#)]
27. Sodano, H.A.; Bae, J.S.; Inman, D.J.; Belvin, W.K. Improved concept and model of eddy current damper. *J. Vib. Acoust.* **2006**, *128*, 294–302. [[CrossRef](#)]
28. Sodano, H.A.; Inman, D.J.; Belvin, W.K. Development of a new passive-active magnetic damper for vibration suppression. *J. Vib. Acoust.* **2006**, *128*, 318–327. [[CrossRef](#)]
29. Sodano, H.A.; Bae, J.S.; Inman, D.J.; Belvin, W.K. Concept and model of eddy current damper for vibration suppression of a beam. *J. Sound Vib.* **2005**, *288*, 1177–1196. [[CrossRef](#)]
30. Bae, J.S.; Kwak, M.K.; Inman, D.J. Vibration suppression of a cantilever beam using eddy current damper. *J. Sound Vib.* **2005**, *284*, 805–824. [[CrossRef](#)]
31. Wang, Z.; Chen, Z.; Wang, J. Feasibility study of a large-scale tuned mass damper with eddy current damping mechanism. *Earthq. Eng. Eng. Vib.* **2012**, *11*, 391–401. [[CrossRef](#)]
32. Larose, G.L.; Larsen, A.; Svensson, E. Modelling of tuned mass dampers for wind-tunnel tests on a full-bridge aeroelastic model. *J. Wind Eng. Ind. Aerodyn.* **1995**, *54*, 427–437. [[CrossRef](#)]
33. Bae, J.S.; Hwang, J.H.; Roh, J.H.; Kim, J.H.; Yi, M.S.; Lim, J.H. Vibration suppression of a cantilever beam using magnetically tuned-mass-damper. *J. Sound Vib.* **2012**, *331*, 5669–5684. [[CrossRef](#)]
34. Bae, J.S.; Hwang, J.H.; Kwag, D.G.; Park, J.; Inman, D.J. Vibration suppression of a large beam structure using tuned mass damper and eddy current damping. *Shock Vib.* **2014**, *2014*, 89314. [[CrossRef](#)]
35. Wen, Q.; Hua, X.G.; Chen, Z.Q.; Yang, Y.; Niu, H.W. Control of Human-Induced Vibrations of a Curved Cable-Stayed Bridge: Design, Implementation, and Field Validation. *J. Bridge Eng.* **2016**, *21*, 04016028. [[CrossRef](#)]
36. Bourquin, F.; Caruso, G.; Peigney, M.; Siegert, D. Magnetically tuned mass dampers for optimal vibration damping of large structures. *Smart Mater. Struct.* **2014**, *23*, 085009. [[CrossRef](#)]
37. Den Hartog, J.P. *Mechanical Vibrations*; Courier Corporation: North Chelmsford, MA, USA, 1985.
38. Rana, R.; Soong, T.T. Parametric study and simplified design of tuned mass dampers. *Eng. Struct.* **1998**, *20*, 193–204. [[CrossRef](#)]
39. Hazra, B.; Sadhu, A.; Lourenco, R.; Narasimhan, S. Re-tuning tuned mass dampers using ambient vibration measurements. *Smart Mater. Struct.* **2010**, *19*, 115002. [[CrossRef](#)]
40. Thompson, A.G. Optimum tuning and damping of a dynamic vibration absorber applied to a force excited and damped primary system. *J. Sound Vib.* **1981**, *77*, 403–415. [[CrossRef](#)]
41. Du, D.; Gu, X.J.; Chu, D.Y.; Hua, H.X. Performance and parametric study of infinite-multiple TMDs for structures under ground acceleration by H_∞ optimization. *J. Sound Vib.* **2007**, *305*, 843–853. [[CrossRef](#)]
42. Zuo, L.; Nayfeh, S.A. Minimax optimization of multi-degree-of-freedom tuned-mass dampers. *J. Sound Vib.* **2004**, *272*, 893–908. [[CrossRef](#)]
43. Asami, T.; Nishihara, O. Closed-form exact solution to H_∞ optimization of dynamic vibration absorbers (application to different transfer functions and damping systems). *J. Vib. Acoust.* **2003**, *125*, 398–405. [[CrossRef](#)]

